

Collective effects in spin-crossover chains with exchange interaction

Carsten Timm*

Institut für Theoretische Physik, Freie Universität Berlin, Arnimallee 14, D-14195 Berlin, Germany

(Dated: August 15, 2005)

The collective properties of spin crossover chains are studied. Spin crossover compounds contain ions with a low-spin ground state and low lying high-spin excited states and are of interest for molecular memory applications. Some of them naturally form one-dimensional chains. Elastic interaction and Ising exchange interaction are taken into account. The transfer-matrix approach is used to calculate the partition function, the fraction of ions in the high-spin state, the magnetization, susceptibility etc. exactly. The high-spin/low-spin degree of freedom leads to collective effects not present in simple spin chains. The ground state phase diagram is mapped out and compared to the case with Heisenberg exchange interaction. The various phases give rise to characteristic behavior at nonzero temperatures, including crossovers between low- and high-temperature regimes, which can become very sharp. A Curie-Weiss law for the susceptibility is derived and the paramagnetic Curie temperature is calculated. Possible experiments to determine the exchange coupling are discussed.

PACS numbers: 75.10.Hk, 75.20.Ck, 75.50.Xx

I. INTRODUCTION

Motivated in part by the search for molecular memory devices,^{1,2,3} spin-crossover compounds (SCCs) have been investigated quite intensively in recent years. These compounds are characterized by magnetic ions that can be either in a low-spin (LS) or high-spin (HS) state, where the HS state is slightly higher in energy and can be thermally populated.^{4,5,6,7,8} An ion in the HS (LS) state has the spin quantum number S_{HS} (S_{LS}), where $S_{\text{HS}} > S_{\text{LS}}$. Most SCCs consist of metal-organic complexes involving transition-metal ions, in many cases Fe^{2+} . Spin crossover involving charge transfer between two different ions is observed in Prussian Blue analogues.^{9,10,11} SCCs are promising for molecular memory applications due to long lifetimes of the HS state. Applications require to deposit SCCs on substrates as thin films or one-dimensional (1D) chains. Many SCCs consist of weakly interacting chains or plains even in the bulk.^{3,12,13,14} A typical quasi-1D material is Fe^{2+} with 4-R-1,2,4-triazole ligands.^{3,13} In this paper we study a 1D spin-crossover model.

SCCs are also interesting from the point of view of basic physics. The additional LS/HS degree of freedom leads to collective effects not present in pure spin models, which are most pronounced for a diamagnetic LS state, $S_{\text{LS}} = 0$, as in the case of Fe^{2+} ions. Then, in the LS state the spin is essentially switched off. This reminds one of diluted spin models,^{15,16,17} but in the SCCs the dilution is not quenched but *fluctuating* in time.

Most of the theoretical literature on SCCs considers models without exchange interaction between the ions. The only interaction in this case is of *elastic* origin and determines whether neighboring ions prefer to be in the same (LS or HS) state or in different ones.^{14,18} However, typical values for the exchange interaction J in transition-metal complex salts are of the order of $|J|/k_B = 10$ to 20 K .^{19,20,21} The interaction is due to superexchange and is typically antiferromagnetic. In fer-

rimagnetic Prussian Blue analogues the exchange interaction is typically similar^{9,10} but values of the order of room temperature have also been reported.²²

If magnetic anisotropies are small, the exchange interaction is of Heisenberg type. For *strong* easy-axis anisotropy, for example due to shape anisotropy of 1D chains, we can consider an Ising exchange interaction. Nishino *et al.*^{23,24,25} and Boukheddaden *et al.*²⁶ study a three-dimensional model with nearest-neighbor Ising exchange, $S_{\text{LS}} = 0$, and $S_{\text{HS}} = 1/2$ (the high spins have two possible orientations) employing mean-field theory and Monte Carlo simulations. On the other hand, Timm and Schollwöck²⁷ consider a 1D model with nearest-neighbor Heisenberg exchange, $S_{\text{LS}} = 0$, and $S_{\text{HS}} = 2$. The *zero-temperature* phase diagram is investigated using the density matrix renormalization group (DMRG).²⁸

In this paper, we study the behavior of the 1D spin-crossover chain with Ising exchange interaction at all temperatures. We will argue that its solution also provides a good approximation for the Heisenberg case for small exchange interactions. In Sec. II we present the model and discuss the transfer-matrix calculations. We mostly restrict ourselves to the case $S_{\text{LS}} = 0$ and $S_{\text{HS}} = 2$, which is appropriate for Fe^{2+} compounds. The results are presented in Secs. III and IV for the ground-state and finite-temperature properties, respectively.

II. MODEL AND METHOD

This section outlines the model and the calculation of equilibrium quantities for general values of S_{HS} , unless stated otherwise. We start from the Hamiltonian

$$H = -V \sum_i \sigma_i \sigma_{i+1} - \Delta \sum_i \sigma_i - J \sum_i m_i m_{i+1} - h \sum_i m_i, \quad (1)$$

where $m_i \equiv S_i^z$ with $m_i = 0$ for $\sigma_i = 1$ (LS state) and $m_i = -S_{\text{HS}}, \dots, S_{\text{HS}}$ for $\sigma_i = -1$ (HS state). Here, V describes the elastic interaction between neighboring

spins.¹⁸ For $V > 0$ ($V < 0$) homogeneous (alternating) arrangements of LS and HS are favored.¹⁴ 2Δ is the energy difference between HS and LS and h is the magnetic field with a factor $g\mu_B$ absorbed. $J > 0$ ($J < 0$) is a ferromagnetic (antiferromagnetic) exchange coupling. For $J = 0$ this model is equivalent to the one of Ref. 29 and for $J = h = 0$ it is the model introduced by Wajnflasz and Pick³⁰ and by Doniach.³¹

We apply the transfer-matrix approach. To focus on the essential physics we assume that the vibrational frequencies of a complex do not change between the LS and HS state. The main effects of different frequencies are to renormalize the energy splitting 2Δ and to change the effective degeneracies of the LS and HS states.^{2,29} These effects do not change the qualitative results and can easily be reintroduced.

The total partition function is

$$Z = \sum_{\{\sigma_i, m_i\}} e^{-\beta H}, \quad (2)$$

where $\beta = 1/T$ (we set $k_B = 1$). We write $-\beta H \equiv \sum_i K_{\sigma_i m_i, \sigma_{i+1} m_{i+1}}$ with

$$K_{\sigma m, \sigma' m'} = \beta V \sigma \sigma' + \frac{\beta \Delta}{2} (\sigma + \sigma') + \beta J m m' + \frac{\beta h}{2} (m + m'). \quad (3)$$

The partition function then reads

$$Z = \sum_{\{\sigma_i, m_i\}} e^{K_{\sigma_1 m_1, \sigma_2 m_2}} e^{K_{\sigma_2 m_2, \sigma_3 m_3}} \dots e^{K_{\sigma_N m_N, \sigma_1 m_1}}. \quad (4)$$

This can be written as $Z = \text{Tr } M^N$ where the symmetric matrix M has the components $M_{\sigma m, \sigma' m'} = \exp(K_{\sigma m, \sigma' m'})$. For $N \rightarrow \infty$ the partition function becomes the maximum eigenvalue of M to the power N and the Gibbs' free energy per site is

$$g = -T \lim_{N \rightarrow \infty} \frac{1}{N} \ln \text{Tr } M^N. \quad (5)$$

For $J = 0$ the eigenvalue equation can be solved in closed form. For $S_{\text{LS}} = 0$ we obtain

$$g = -\frac{1}{\beta} \ln \left(e^{\beta V} \cosh \beta \tilde{\Delta} + \sqrt{e^{2\beta V} \sinh^2 \beta \tilde{\Delta} + e^{-2\beta V}} \right) - \frac{\ln g_{\text{HS}}}{2\beta} \quad (6)$$

with $\tilde{\Delta} \equiv \Delta - \ln g_{\text{HS}}/2\beta$ and²⁹

$$g_{\text{HS}} \equiv \sum_{m=-S_{\text{HS}}}^{S_{\text{HS}}} e^{\beta h m} = \frac{e^{\beta h (S_{\text{HS}} + 1/2)} - e^{-\beta h (S_{\text{HS}} + 1/2)}}{e^{\beta h/2} - e^{-\beta h/2}}. \quad (7)$$

For $h = 0$ one has $g_{\text{HS}} = 2S_{\text{HS}} + 1$.

For $J \neq 0$, $S_{\text{LS}} = 0$, $S_{\text{HS}} = 2$ the calculation of the partition function has been reduced to the eigenvalue problem of a 6×6 matrix. An important quantity describing

SCCs is the fraction γ of ions in the HS state. It is given by $\gamma = (1 - \langle \sigma \rangle)/2$ so that, with Eq. (6),

$$\gamma = \frac{1 + \partial g / \partial \Delta}{2} = \frac{1}{2} - \frac{T}{2} \lim_{N \rightarrow \infty} \frac{\text{Tr } M^{N-1} \partial M / \partial \Delta}{\text{Tr } M^N}. \quad (8)$$

If $|n\rangle$, $n = 1, \dots, 6$ are the orthonormalized eigenvectors of M with eigenvalues $m_1 \geq m_2 \geq \dots \geq m_6$, then

$$\gamma = \frac{1}{2} - \frac{T}{2} \frac{\langle 1 | \partial M / \partial \Delta | 1 \rangle}{m_1}. \quad (9)$$

The components of $\partial M / \partial \Delta$ are easily obtained from M . Similarly, the magnetization is

$$\langle m \rangle = -\frac{\partial g}{\partial h} = T \frac{\langle 1 | \partial M / \partial h | 1 \rangle}{m_1} \quad (10)$$

and the probability of any two neighbors being in the same (LS or HS) state is

$$w_{\text{eq}} = \frac{1 - \partial g / \partial V}{2} = \frac{1}{2} + \frac{T}{2} \frac{\langle 1 | \partial M / \partial V | 1 \rangle}{m_1}. \quad (11)$$

These quantities will be of importance later.

For $J = 0$ we find the HS fraction

$$\gamma = \frac{1}{2} - \frac{1}{2} \frac{e^{\beta V} \sinh \beta \tilde{\Delta}}{\sqrt{e^{2\beta V} \sinh^2 \beta \tilde{\Delta} + e^{-2\beta V}}}. \quad (12)$$

In this case the magnetization is determined by γ through $\langle m \rangle = \gamma S_{\text{HS}} B_{S_{\text{HS}}}(\beta h S_{\text{HS}})$, where $B_S(x)$ is the Brillouin function. This leads to a simple result for the susceptibility $\chi = \partial \langle m \rangle / \partial h$ for vanishing magnetic field:

$$\chi = \gamma \frac{S_{\text{HS}}(S_{\text{HS}} + 1)}{3T}. \quad (13)$$

Thus the susceptibility is just the paramagnetic expression weighted by the concentration of high spins.

III. GROUND STATES

In this section we derive the ground-state phase diagram of the spin-crossover chain to lay the ground for the discussion of finite-temperature properties. For the case without exchange interaction, $J = 0$, Fig. 1 shows the phase diagram in terms of the two dimensionless ratios V/Δ and h/Δ . From Eq. (6) we find $\gamma = 0$, $\langle m \rangle = 0$, and $w_{\text{eq}} = 1$ for $|h|/\Delta < 2/S_{\text{HS}}$ and $V/\Delta > -1/2 + |h|S_{\text{HS}}/4\Delta$. This is the LS state. For $|h|/\Delta > 2/S_{\text{HS}}$ and $V/\Delta > 1/2 - |h|S_{\text{HS}}/4\Delta$ we find $\gamma = 1$, $\langle m \rangle = S_{\text{HS}} \text{sgn } h$, and $w_{\text{eq}} = 1$. This is the fully polarized HS state. In all other cases we find $\gamma = 1/2$, $\langle m \rangle = S_{\text{HS}} \text{sgn } h/2$, and $w_{\text{eq}} = 0$, corresponding to an alternating state of LS and HS ions.

In the general case with Ising exchange interaction we have three dimensionless parameters, V/Δ , J/Δ , and h/Δ . The ground state for given parameters is found by

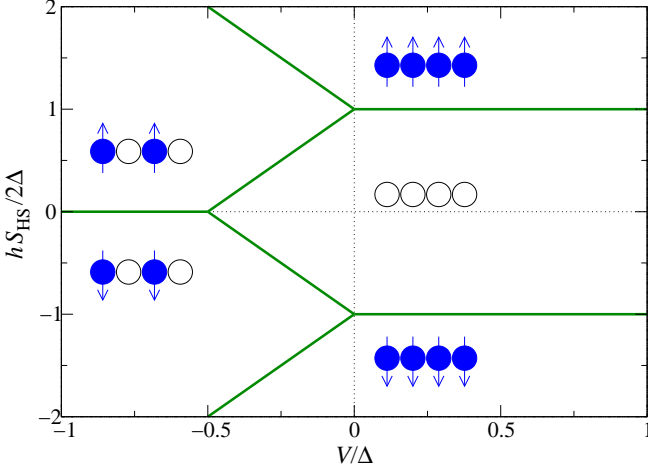


FIG. 1: (Color online) Ground-state phase diagram of the 1D spin-crossover model without exchange interaction and with $S_{LS} = 0$, in terms of elastic interaction V and Zeeman energy h in units of Δ , where 2Δ is the LS/HS energy splitting. The solid lines denote discontinuous transitions.

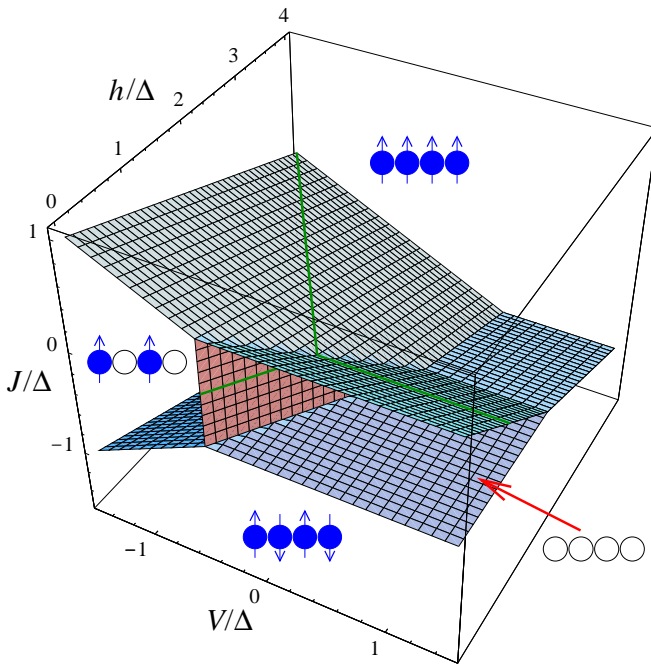


FIG. 2: (Color online) Ground-state phase diagram of the 1D spin-crossover chain with Ising exchange coupling J . In this and the following graphs $S_{LS} = 0$ and $S_{HS} = 2$ are assumed. The planes denote discontinuous transitions. The heavy solid lines show their intersections with the $J = 0$ plane, see Fig. 1.

determining the largest component(s) of the matrix M , since for $T \rightarrow 0$ these components become exponentially larger than the others. For sufficiently large $J/\Delta > 0$ we obtain a ferromagnetically aligned HS phase for any V, h . This is similar to the exchange-induced ferromagnetism in rare-earth compounds.³² For $S_{HS} = 2$ and $h \geq 0$ this

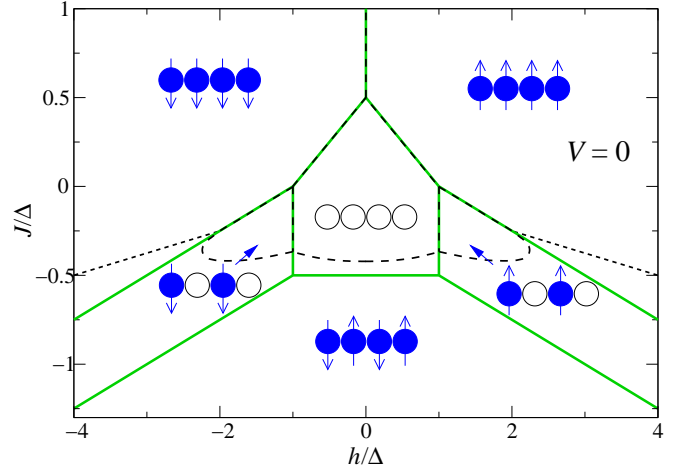


FIG. 3: (Color online) Solid lines: Intersection of the $T = 0$ phase diagram, Fig. 2, with the $V = 0$ plane (vanishing elastic interaction). Dashed curves: The phase boundaries for Heisenberg exchange interaction.²⁷ Long-dashed (short-dashed) curves correspond to discontinuous (continuous) transitions. The alternating phase is reduced to two finite lobes by quantum effects. The more complex phases of the Heisenberg-type model only appear at $V < 0$. Note that the phase boundaries for the Ising- and Heisenberg-type models are identical for positive and small negative J .

phase becomes unstable at

$$\frac{J}{\Delta} = \begin{cases} -\frac{h}{2\Delta} + \frac{1}{2} & \text{for } \frac{h}{\Delta} < 2 \wedge \frac{V}{\Delta} > \frac{h}{2\Delta} - \frac{1}{2} \\ -\frac{V}{2\Delta} - \frac{h}{4\Delta} + \frac{1}{4} & \begin{cases} \text{for } \frac{h}{\Delta} < 2 \wedge \frac{V}{\Delta} < \frac{h}{2\Delta} - \frac{1}{2} \\ \text{for } \frac{h}{\Delta} > 2 \wedge \frac{V}{\Delta} < \frac{1}{2} \end{cases} \\ -\frac{h}{4\Delta} & \text{for } \frac{h}{\Delta} > 2 \wedge \frac{V}{\Delta} > \frac{1}{2}. \end{cases} \quad (14)$$

For large $-J/\Delta > 0$ we find a HS phase with Néel order, which does not exist for $J = 0$. It becomes unstable at

$$\frac{J}{\Delta} = \begin{cases} -\frac{1}{2} & \text{for } \frac{h}{\Delta} < 2 \wedge \frac{V}{\Delta} > \frac{h}{2\Delta} - \frac{1}{2} \\ \frac{V}{2\Delta} - \frac{h}{4\Delta} - \frac{1}{4} & \begin{cases} \text{for } \frac{h}{\Delta} < 2 \wedge \frac{V}{\Delta} < \frac{h}{2\Delta} - \frac{1}{2} \\ \text{for } \frac{h}{\Delta} > 2 \wedge \frac{V}{\Delta} < \frac{1}{2} \end{cases} \\ -\frac{h}{4\Delta} & \text{for } \frac{h}{\Delta} > 2 \wedge \frac{V}{\Delta} > \frac{1}{2}. \end{cases} \quad (15)$$

Finally, for small $|J/\Delta|$ the LS and alternating phases are separated by a boundary at

$$\frac{V}{\Delta} = \frac{h}{2\Delta} - \frac{1}{2} \quad \text{for } -\frac{1}{2} < \frac{J}{\Delta} < \frac{1}{2} - \frac{h}{2\Delta}. \quad (16)$$

The resulting $T = 0$ phase diagram is shown in Fig. 2. Figure 3 shows the $V = 0$ cut of the phase diagram and compares the results to the case of Heisenberg exchange interaction from Ref. 27. In the Ising case the more

complex phases of the Heisenberg-type model are absent, which consist of magnetic unit cells of $n = 2, 3, 5, 7, 9$ ions in the HS state and a single ion in the LS state.²⁷ These phases are stabilized in the Heisenberg case by the energy gain in antiferromagnetically coupled spin chains due to quantum effects. This energy gain also stabilizes the antiferromagnetically aligned HS state, which displaces the other phases, as seen in Fig. 3.

On the other hand, for all positive and small negative J/Δ the phase boundaries coincide. This is because the ground states of the Ising-type model remain eigenstates of the Heisenberg-type model with the same energy and all ground states that appear at larger $-J$ have nonzero energy gaps to the ground state at small $|J|$. Thus for small $|J|$ no new phases appear for either the Ising or the Heisenberg case and both have the same ground states. In most SCCs we expect $|J|$ to be small and the Ising-type model gives the exact ground state even for isotropic exchange interaction.

IV. FINITE-TEMPERATURE BEHAVIOR

We now turn to the properties of the spin-crossover chain at finite temperatures. The partition function is analytic for $T > 0$ so that there are no phase transitions. However, they are replaced by crossovers, which can become very sharp.

The assumption of Ising exchange provides a reasonable approximation also for the Heisenberg case for small exchange interaction. For small J the ground state is found exactly and the energies of low-lying excited states above the LS and alternating ground states are also identical for both cases so that the behavior at low $T > 0$ will be very similar. On the other hand, in the ferromagnetic HS state the low-energy excitations are different but gapped in both cases. Thus only qualitatively similar behavior is expected.³³

A. Low-spin phase

Typical SCCs are in the LS phase for $T \rightarrow 0$. Figure 4 shows the HS fraction as a function of temperature for $J = 0$ and various elastic interaction strengths V . For $V = 0$ we observe the well-known smooth crossover to the HS state, which comes from its higher degeneracy. For $T \rightarrow \infty$ the HS fraction is only determined by the degeneracies, $\gamma \rightarrow (2S_{\text{HS}} + 1)/(2S_{\text{HS}} + 2) = 5/6$ (this holds for any V). For $V > 0$ the interaction favors a homogeneous state and the crossover becomes *sharper*. In mean-field theory we would eventually reach a critical point $V = V_c$ and find a discontinuous transition for $V > V_c$.³ In 1D γ develops a discontinuity only for $V \rightarrow \infty$. For larger V/Δ the curves *overshoot* and exhibit a maximum. This is due to the energy gain from the homogeneous HS state outweighing the entropy gain from populating all states equally. For $V < 0$, but still in the LS phase at $T \rightarrow 0$,

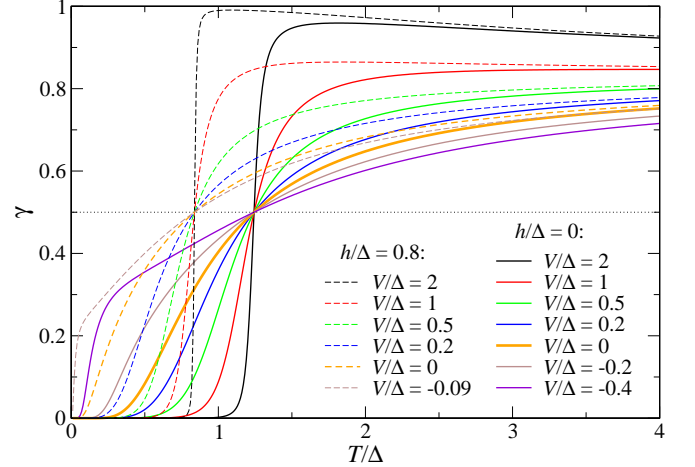


FIG. 4: (Color online) Solid curves: HS fraction γ as a function of temperature for various values of the elastic interaction V and vanishing magnetic field. Dashed curves: γ for $h/\Delta = 0.8$. The state at $T = 0$ is in the LS phase.

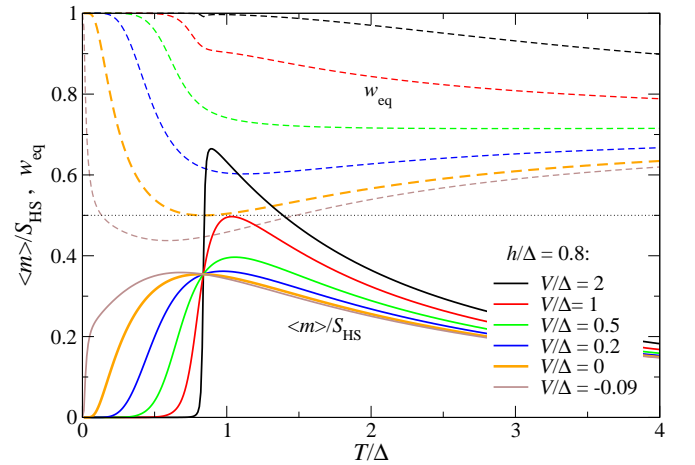


FIG. 5: (Color online) Solid curves: Magnetization $\langle m \rangle / S_{\text{HS}}$ as a function of temperature for various values of the elastic interaction V and Zeeman energy $h/\Delta = 0.8$. Dashed curves of same color: Probability w_{eq} of neighboring ions being in the same (LS or HS) state for the same parameters. The state at $T = 0$ is in the LS phase.

the interaction favors a mixed state with $\gamma \approx 1/2$ and thus broadens the crossover.

All curves for fixed h in Fig. 4 cross at $\gamma = 1/2$. The equation $\gamma(T_\gamma) = 1/2$ is equivalent to $\langle \sigma \rangle = 0$ and, using Eq. (12), to $\Delta - (T/2) \ln g_{\text{HS}} = 0$. This leads to the implicit equation $T_\gamma/\Delta = 2/\ln g_{\text{HS}}(h, T_\gamma)$, which is indeed independent of the interaction V so that all curves cross at T_γ . For $h = 0$ we obtain $T_\gamma/\Delta = 2/\ln(2S_{\text{HS}} + 1)$.

The magnetization $\langle m \rangle$ and probability w_{eq} for equal neighbors are shown in Fig. 5 for $h/\Delta = 0.8$. For $V = 0$ we see a broad crossover in $\langle m \rangle$ from the LS phase to a maximum and then a decay $\sim 1/T$ at high temperatures. The Curie-Weiss law is discussed further in Sec. IV C. For $V > 0$ ($V < 0$) the crossover becomes sharper (broader).

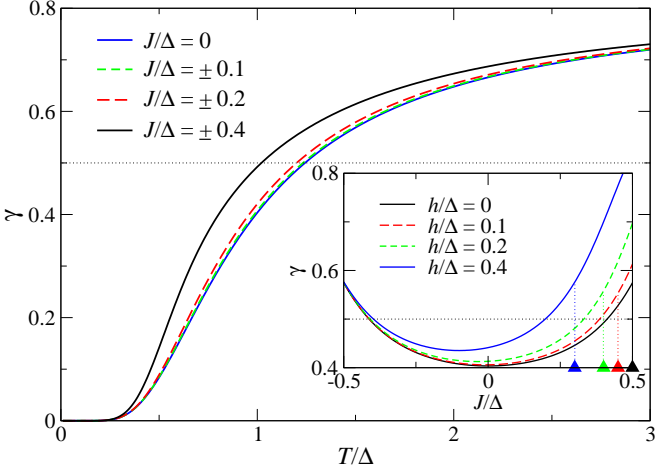


FIG. 6: (Color online) HS fraction γ as a function of temperature for various values of the exchange interaction J and $V = h = 0$. Inset: HS fraction γ as a function of exchange interaction J/Δ for various values of the Zeeman energy h for $T/\Delta = 1$ and $V = 0$. The $T = 0$ transition between LS and antiferromagnetic HS phases is at $J/\Delta = -1/2$, the positions of the transitions to the ferromagnetic HS phase are marked by triangles of the same color as the corresponding curves.

Similar behavior is found for $J \neq 0$. The nonmonotonic temperature dependence can be interpreted as the 1D analogon of the reentrant transition to ferromagnetic order found in three dimensions.²⁶

The probability w_{eq} starts from $w_{\text{eq}} = 1$ at $T = 0$ and approaches a universal value of $13/18$ for $T \rightarrow \infty$. w_{eq} shows a broad minimum for small V and a small but sharp feature at the crossover for large V . The minimum is best understood in the case without interactions. Then $w_{\text{eq}} = \gamma^2 + (1 - \gamma)^2$ so that $\gamma = 1/2$ implies $w_{\text{eq}} = 1/2$, which is smaller than the limits for low and high T .

Next, we consider the effect of the exchange interaction. Figure 6 shows the HS fraction for various values of J . For vanishing magnetic field the effect of moderate $|J/\Delta|$ is rather weak due to the scarcity of nearest-neighbor HS pairs. For $J \neq 0$ the crossover temperature with $\gamma(T_\gamma) = 1/2$ depends on both J and V . γ increases *symmetrically* for ferromagnetic and antiferromagnetic J for all V , due to the invariance of the Hamiltonian under $m_i \rightarrow (-1)^i m_i$ and $J \rightarrow -J$ for $h = 0$. The $T = 0$ transitions to the ferromagnetic and antiferromagnetic HS phases take place at $J/\Delta = \pm 1/2$, respectively. For $h \neq 0$ the transition to the ferromagnetic phase shifts to lower values of J , whereas the antiferromagnetic transition remains fixed, see Fig. 3, so that the minimum of $\gamma(J)$ shifts to lower J .

B. Other phases

The alternating LS/HS phase is stabilized by a strongly negative elastic interaction V .¹⁴ This can be expected for SCCs grown on a substrate, where the transition of an

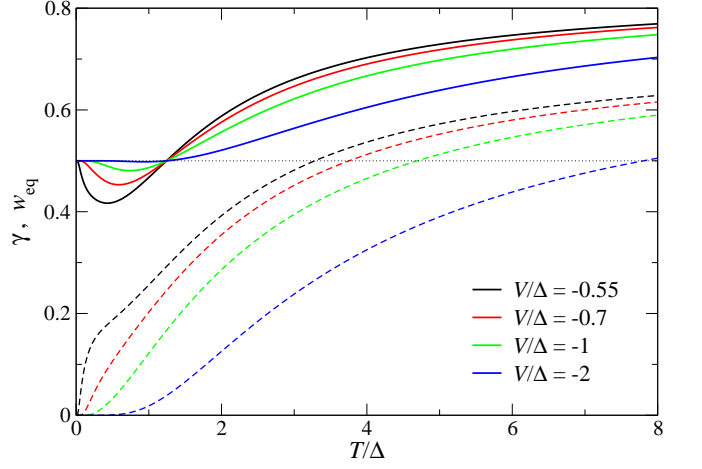


FIG. 7: (Color online) HS fraction γ (solid curves) and probability w_{eq} of neighbors being in the same state (dashed curves of same color) as functions of temperature for various values of the elastic interaction V and $J = h = 0$. The state at $T = 0$ is in the alternating LS/HS phase.

ion to the HS state increases its radius, which should favor a smaller ionic radius (LS state) of its neighbors.

Figure 7 shows the HS fraction and the probability of neighbors in the same state for $J = h = 0$. γ first decreases with temperature and shows a universal crossing at $\gamma = 1/2$ and $T = T_\gamma$ as in the LS phase. The HS fraction first decreases since the alternating order is partially destroyed (w_{eq} increases) and the energy of spins having one LS and one HS neighbor is only determined by Δ , which favors the LS state. The effect of a nonzero exchange interaction J is weak, as long as J and Zeeman energy h are not so large that the system approaches a phase transition at $T \rightarrow 0$ (not shown). At zero field γ is again an even function of J .

While the exchange interaction only has a weak effect in the LS and alternating phases, the situation changes for the HS phases. The *ferromagnetically* aligned phase appears at (very strong) magnetic fields and for strong ferromagnetic exchange interaction—both might not be realized in SCCs. Typical results for the field-induced ferromagnetic HS state are shown in Fig. 8. γ goes through a minimum since the ground state of a single ion would be the lowest state of the HS quintet, while the first excited state is the LS singlet. Therefore for increasing temperature the LS state contributes first. The magnetization is determined by γ and a Brillouin function containing the external field, as noted in Sec. II.

For the ferromagnetic phase induced by strong exchange J at small field, Fig. 9 shows typical results for the HS fraction and magnetization. γ and $\langle m \rangle$ now depend *strongly* on J . The HS fraction behaves similarly to the case of $J = 0$ and large field but now the simple relation between HS fraction and magnetization no longer holds—it would predict a tiny magnetization at $h/\Delta = 10^{-2}$. Instead, the magnetization shows a rather

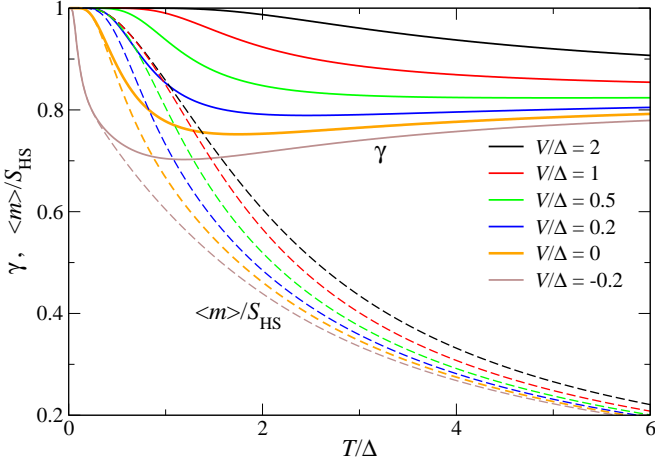


FIG. 8: (Color online) HS fraction γ (solid curves) and magnetization $\langle m \rangle$ (dashed curves of same color) as functions of temperature for various values of the elastic interaction V , $J = 0$, and $h/\Delta = 1.5$. The state at $T = 0$ is in the HS phase.

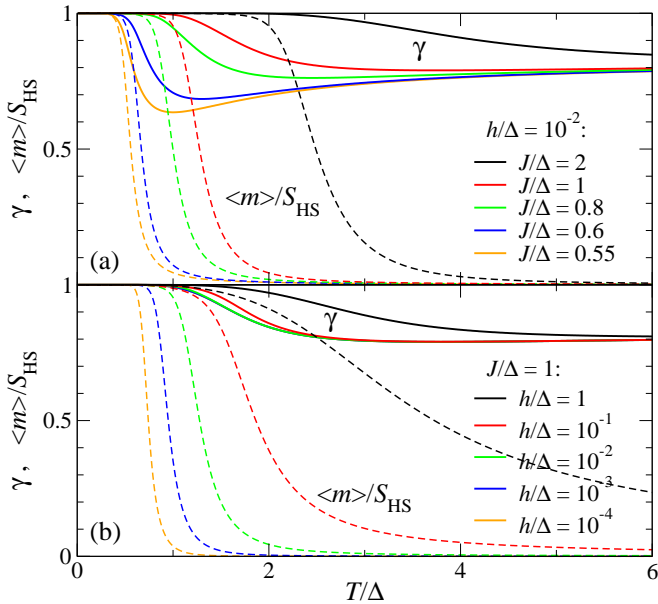


FIG. 9: (Color online) (a) HS fraction γ (solid curves) and magnetization $\langle m \rangle$ (dashed curves of same color) as functions of temperature for various values of the exchange interaction J , $V = 0$, and small $h/\Delta = 10^{-2}$. (b) The same for fixed $J/\Delta = 1$ and various Zeeman energies. The state at $T = 0$ is in the ferromagnetic HS phase.

sharp crossover from nearly full polarization to low magnetization. Figure 9(b) shows the dependence of γ and $\langle m \rangle$ on magnetic field. At small $h/\Delta \lesssim 10^{-2}$ the HS fraction hardly depends on h , but the magnetization shows a strong field dependence. There is a strong tendency towards ferromagnetic order even at very small h , whereas the magnetization vanishes for $h = 0$. We return to this crossover in Sec. IV D.

Finally, the *antiferromagnetically* aligned HS phase

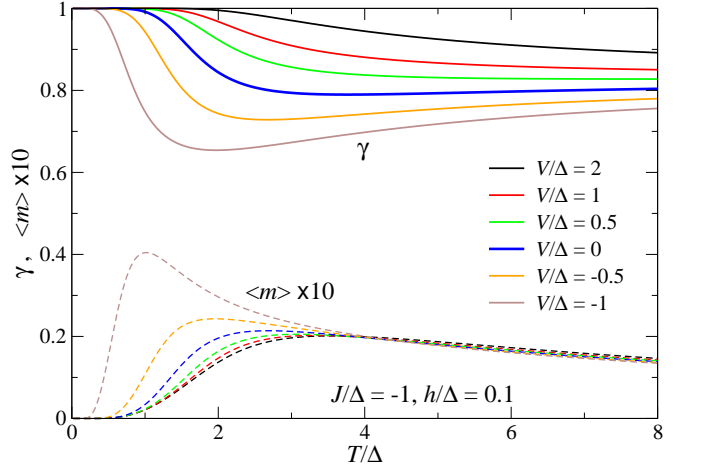


FIG. 10: (Color online) High-spin fraction γ (solid curves) and magnetization $\langle m \rangle$ (dashed curves of same color, scaled by 10) as functions of temperature for various values of the elastic interaction V , $h/\Delta = 0.1$, and $J/\Delta = -1$. The state at $T = 0$ is in the antiferromagnetic HS phase.

only exists for strong antiferromagnetic exchange $J/\Delta < -1/2$. Figure 10 shows the HS fraction and the magnetization for fixed $J/\Delta = -1$ in a magnetic field. γ behaves very similarly to the ferromagnetic phase, Fig. 8. The field induces a nonzero magnetization only for $T > 0$ because of the energy gap for spin flips. For Heisenberg exchange the temperature dependence would be quite different: The ground state in that case still has $\gamma = 1$ but no long-range order due to transverse spin fluctuations. However, it is also gapped since S_{HS} is an integer.³⁴

C. High-temperature limit

In the present subsection we consider the high-temperature expansion of thermodynamic quantities. We discuss the Curie-Weiss law for the susceptibility and possible experiments to determine the exchange coupling.

In Sec. II the partition function z for a single site has been obtained as the largest eigenvalue of the matrix M . We write $M = M_\infty + \Delta M$ with $(M_\infty)_{\sigma m, \sigma' m'} \equiv \lim_{T \rightarrow \infty} M_{\sigma m, \sigma' m'} = 1$ and calculate z perturbatively for small ΔM . M_∞ has an eigenstate $|1\rangle_0 = (1, 1, 1, 1, 1, 1)/\sqrt{6}$ with eigenvalue $2S_{\text{HS}} + 2 = 6$ and all other eigenvalues vanish. Using standard perturbation theory for z and the corresponding eigenstate $|1\rangle$ and expanding in $1/T$ we obtain

$$\begin{aligned} z \cong 6 + & \frac{8V - 12\Delta}{3T} \\ & + \frac{121V^2 - 168V\Delta + 81\Delta^2 + 225J^2 + 135h^2}{27T^2} \\ & + (148V^3 - 846V^2\Delta + 774V\Delta^2 + 2925VJ^2 \\ & + 1080Vh^2 - 162\Delta^3 - 2700\Delta J^2 - 1215\Delta h^2 \\ & + 4050Jh^2)/(243T^3) + \mathcal{O}(1/T^4). \end{aligned} \quad (17)$$

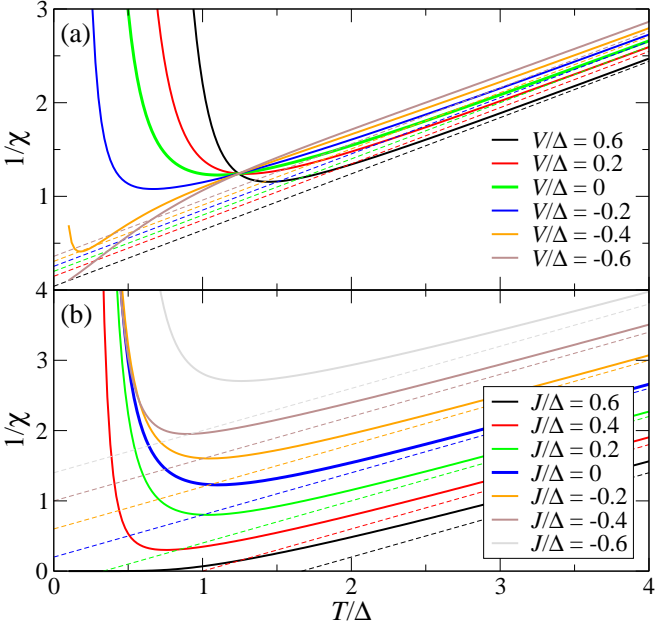


FIG. 11: (Color online) Inverse susceptibility $1/\chi$ as a function of temperature for vanishing magnetic field, $h = 0$. (a) For $J = 0$ and various values of V/Δ . (b) For $V = 0$ and various values of J/Δ . The solid curves show the exact results, while the dashed curves of the same color give the Curie-Weiss law $\chi \cong 5/(3(T - \Theta))$ with Θ given by Eq. (20).

The Gibbs' free energy per site is then $g = -T \ln z$ and the susceptibility is

$$\chi = -\frac{\partial^2 g}{\partial h^2} \cong \frac{5}{3T} + \frac{5(4V - 3\Delta + 30J)}{27T^2} + \mathcal{O}(1/T^3). \quad (18)$$

Expanding the Curie-Weiss law $\chi = C/(T - \Theta)$ we find

$$\chi \cong \frac{5}{3} \frac{1}{T - \Theta} \quad (19)$$

with the paramagnetic Curie temperature

$$\Theta = \frac{4V - 3\Delta + 30J}{9}. \quad (20)$$

Figure 11 shows the approach of the exact result for $1/\chi$ to the Curie-Weiss form.

We see that the high-temperature behavior of the susceptibility not only depends on the exchange interaction J but also on the elastic interaction and the LS/HS energy splitting. Interestingly, the paramagnetic Curie temperature Θ is nonzero even without *any* interaction, in which case $\Theta = -\Delta/3$. Thus there is a deviation from the Curie law for the susceptibility of *noninteracting* spin-crossover ions. The reason is that the ground state is diamagnetic and thermal activation with $T \sim \Delta$ is required to make an ion paramagnetic. Obviously, $\Theta < 0$ does not imply an antiferromagnetic ground state. Similarly, the ground state is not always ferromagnetic if $\Theta > 0$ —the tendency towards ferromagnetism is then preempted by the crossover to the LS state.

Since it is difficult to infer the value or even the sign of J from the paramagnetic Curie temperature, we propose another route to extract J . For $J = h = 0$ we have $\chi = 2\gamma/T$, cf. Eq. (13). This identity does not hold for nonzero J so that the *deviation* from it might be a good measure of J . We thus consider the ratio $\mu \equiv \chi T/2\gamma$ at vanishing magnetic field. From Eq. (17) we obtain

$$\gamma = \frac{1 + \partial g/\partial \Delta}{2} \cong \frac{5}{6} + \frac{5(4V - 3\Delta)}{54T} + \mathcal{O}(1/T^2) \quad (21)$$

and, at $h = 0$,

$$\mu = \frac{-T \partial^2 g/\partial h^2}{1 + \partial g/\partial \Delta} \cong 1 + \frac{10J}{3T} + \mathcal{O}(1/T^2). \quad (22)$$

The leading high-temperature behavior of μ is entirely determined by J . This suggests that the effect of V and Δ on the high-temperature susceptibility only comes from the HS fraction. Numerical results suggest that $\mu > 1$ ($\mu < 1$) for $J > 0$ ($J < 0$) at *all* temperatures. Since both χ and γ are, in principle, measurable quantities, μ is a promising quantity for the determination of the exchange coupling.

D. Finite-temperature crossovers

The finite-temperature crossovers found in the preceding subsections are now studied in more detail. Regardless of the specific ground state, for high temperatures the system approaches a limit with $\gamma = 5/6$, $\langle m \rangle = 0$, and $w_{\text{eq}} = \gamma^2 + (1 - \gamma)^2 = 13/18$. If one starts from the LS ground state, γ has to go from zero to $5/6$. Figures 4 and 6 suggest that $\gamma(T_\gamma) = 1/2$ is a good condition for the characteristic crossover temperature T_γ . Starting from the alternating phase with $\gamma = 1/2$, γ first drops and then recrosses $\gamma = 1/2$, at least for small J , see Fig. 7. Another measure of the crossover from the alternating phase is the probability of neighbors in the same state being $w_{\text{eq}}(T_w) = 1/2$.

We first consider the case $J = 0$. Equation (12) shows that $\gamma(T_\gamma) = 1/2$ is equivalent to $\tilde{\Delta} = 0$. T_γ becomes zero for $|h|/\Delta = 2/S_{\text{HS}} = 1$. There is nontrivial solution only for $|h|/\Delta < 1$, i.e., in the LS and *part of* the alternating phase. Note that T_γ is independent of V . The equation $w_{\text{eq}}(T_w) = 1/2$ has *two* solutions (reentrance) for the part of the LS phase with $V < 0$, cf. Fig. 5, whereas it has only one solution for the alternating phase and none for $V > 0$. T_w goes to zero at the phase boundaries involving the alternating ground state. Figure 12 shows the crossover temperatures. The LS state is destroyed by temperatures $T \sim 2\Delta$, the energy per ion for going from the LS to the HS state. On the other hand, the alternating state is stable up to $T \sim 2|J|$, the energy cost for breaking LS/HS pairs.

For $J \neq 0$ the typical behavior can already be seen for the case of vanishing elastic interaction. Figures 13(a,b) show the crossover temperatures defined by $\gamma = 1/2$ and

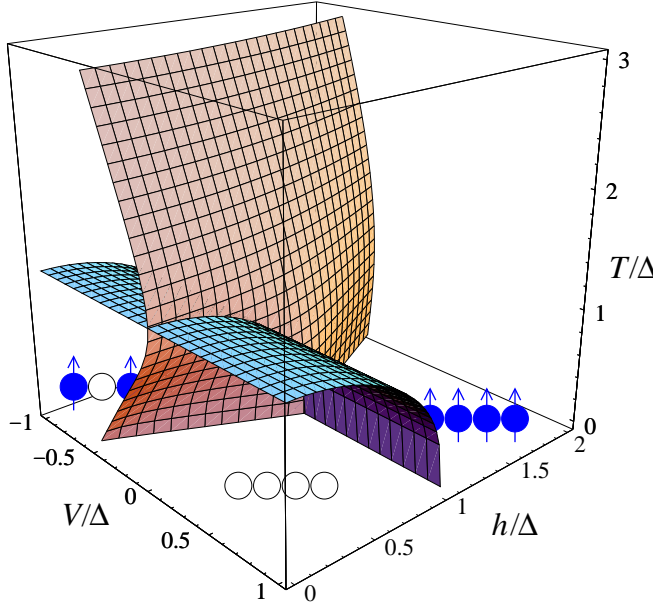


FIG. 12: (Color online) Crossover temperatures for $J = 0$. The $T = 0$ plane corresponds to Fig. 1. The surfaces indicate solutions of $\gamma = 1/2$ and $w_{\text{eq}} = 1/2$, respectively.

$w_{\text{eq}} = 1/2$ as functions of h/Δ and J/Δ . This should be compared to the phase diagram in Fig. 3. The reentrant behavior in Fig. 13(b) is continuously connected to the two solutions found in Fig. 12.

For the alternating ground state we find that there is (at least) one nonzero temperature with $\gamma = 1/2$ for *some* parameter values, as in the $J = 0$ case. The parameter range where this is the case narrows and vanishes for fields above $h/\Delta \approx 2.27$, as seen in Fig. 13(a).

The crossover from the ferromagnetic HS ground state to the high-temperature HS state with $\langle m \rangle = 0$ is characterized by the condition $\langle m \rangle = S_{\text{HS}}/2$. The crossover becomes very sharp at low magnetic field, cf. Fig. 9. Figure 13(c) shows the crossover temperature for $V = 0$, which depends *logarithmically* on magnetic field for small h . This result is known from the 1D Ising model and can be understood from the formation energy of droplets of reduced spin polarization.

V. SUMMARY

The thermodynamic properties of 1D SCCs with nearest-neighbor elastic and Ising exchange interactions have been investigated using the exact transfer-matrix approach. This is motivated by SCCs naturally forming 1D chains, like Fe^{2+} with 4-R-1,2,4-triazole ligands, and by possible artificial 1D structures for molecular electronics. The HS fraction, magnetization, and spin susceptibility are calculated, as well as the probability of neighboring ions being in the same (LS or HS) state. The knowledge of these quantities allows one to map out the $T = 0$ phase diagram. A strong magnetic field or a ferromagnetic ex-

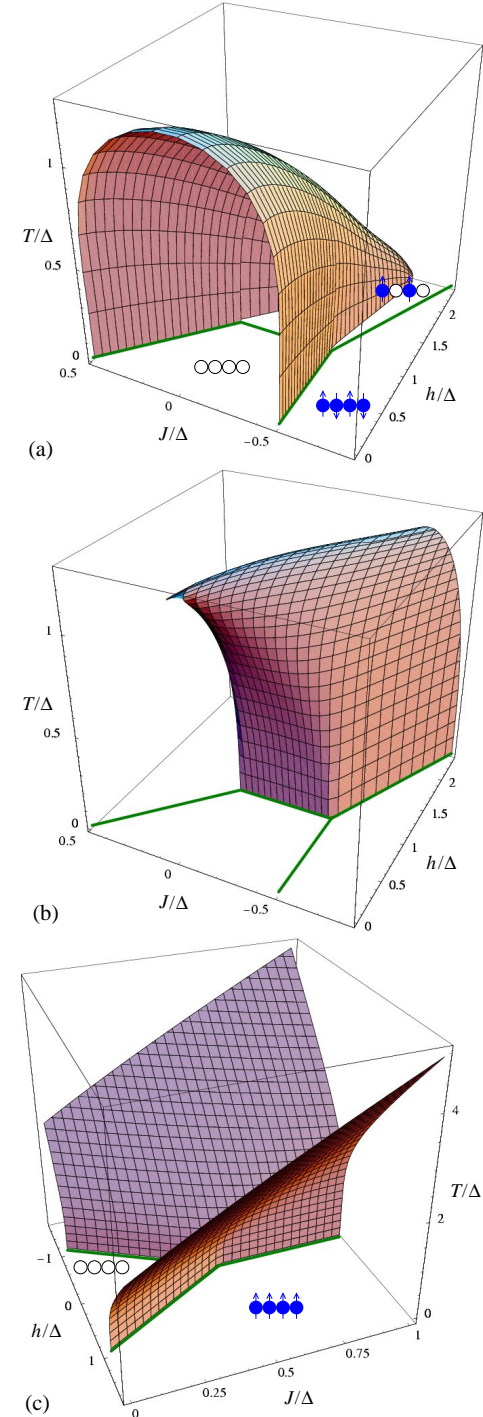


FIG. 13: (Color online) Crossover temperatures for $V = 0$, defined by (a) $\gamma = 1/2$, (b) $w_{\text{eq}} = 1/2$, (c) $\langle m \rangle/S_{\text{HS}} = 1/2$. The $T = 0$ plane corresponds to Fig. 3. Phase boundaries at $T = 0$ are marked by heavy solid lines.

change interaction can drive the system into a ferromagnetically aligned HS ground state, whereas an antiferromagnetic exchange interaction can lead to an antiferromagnetically aligned ground state. A negative elastic interaction can drive the system into an alternating LS/HS

ground state. These phases give rise to characteristically different behavior at finite temperatures. Nonmonotonic temperature dependence of HS fraction and magnetization are ubiquitous. While there are no phase transitions at $T > 0$, the crossovers between the low-temperature behavior and the HS-dominated high-temperature limit can become very sharp. Spin crossover chains show 1D analogs of the interesting effects found in the bulk, such as reentrant transitions²⁶ and stripe phases.¹⁴

The susceptibility follows the Curie-Weiss law at high temperatures for all ground-state phases. The paramagnetic Curie temperature is found to depend not only on the exchange interaction but also on elastic interaction and LS/HS energy splitting. It is nonzero even for noninteracting complexes. The exchange coupling J could be determined experimentally from the susceptibility χ and HS fraction γ using that the high-temperature behavior of the ratio $\chi T/2\gamma$ depends only on J .

The typical energy scale in all results is Δ , half the LS/HS energy splitting for a single ion. It would thus be desirable to tune this scale to *small* values by a suitable choice of ligands so that *large* values of the dimensionless parameters V/Δ , J/Δ , and h/Δ can be reached. This would allow to test the rich temperature-dependent effects predicted here.

Acknowledgments

I would like to thank P. J. Jensen for valuable discussions. Support by the Deutsche Forschungsgemeinschaft through Sonderforschungsbereich 658, *Elementary processes in molecular switches on surfaces*, is gratefully acknowledged.

* Electronic address: timm@physik.fu-berlin.de

- ¹ J. Zarembowitch and O. Kahn, *New J. Chem.* **15**, 181 (1991); O. Kahn, J. Kröber, and C. Jay, *Advan. Mater.* **4**, 718 (1992).
- ² H. Bolvin and O. Kahn, *Chem. Phys.* **192**, 295 (1995); *Chem. Phys. Lett.* **243**, 355 (1995).
- ³ O. Kahn and C. Jay Martinez, *Science* **279**, 44 (1998).
- ⁴ L. Cambi and L. Szegö, *Ber. Dtsch. Chem. Ges.* **64**, 259 (1931); **66**, 656 (1933).
- ⁵ P. Gütlich, *Struct. Bonding (Berlin)* **44**, 83 (1981).
- ⁶ E. König, *Struct. Bonding (Berlin)* **76**, 51 (1991).
- ⁷ P. Gütlich, Y. Garcia, and H. A. Goodwin, *Chem. Soc. Rev.* **29**, 419 (2000).
- ⁸ S. J. Blundell and F. L. Pratt, *J. Phys.: Condens. Matter* **16**, R771 (2004).
- ⁹ O. Sato, T. Iyoda, A. Fujishima, and K. Hashimoto, *Science* **272**, 704 (1996).
- ¹⁰ A. Goujon, O. Roubeau, M. Noguès, F. Varret, A. Dolbecq, M. Verdaguer, *Eur. Phys. J. B* **14**, 115 (2000).
- ¹¹ A. Bleuzen, C. Lomenech, V. Escax, F. Villain, F. Varret, C. Cartier dit Moulin, and M. Verdaguer, *J. Am. Chem. Soc.* **122**, 6648 (2000).
- ¹² M. Coutanceau, P. Dordor, J.-P. Doumerc, J.-C. Grenier, P. Maestro, M. Pouchard, D. Sedmidubsky, and T. Seguelong, *Solid State Commun.* **96**, 569 (1995); J.-P. Doumerc, J.-C. Grenier, P. Hagenmuller, M. Pouchard, and A. Villesuzanne, *J. Solid State Chem.* **147**, 211 (1999); J.-P. Doumerc, M. Coutanceau, A. Demourgues, E. Elkaim, J.-C. Grenier, and M. Pouchard, *J. Mater. Chem.* **11**, 78 (2001).
- ¹³ T. Yokoyama, Y. Murakami, M. Kiguchi, T. Komatsu, and N. Kojima, *Phys. Rev. B* **58**, 14238 (1998).
- ¹⁴ D. I. Khomskii and U. Löw, *Phys. Rev. B* **69**, 184401 (2004).
- ¹⁵ O. P. Vajk, P. K. Mang, M. Greven, P. M. Gehring, and J. W. Lynn, *Science* **295**, 1691 (2002).
- ¹⁶ K. Kato, S. Todo, K. Harada, N. Kawashima, S. Miyashita, and H. Takayama, *Phys. Rev. Lett.* **84**, 4204 (2000); A. W. Sandvik, *Phys. Rev. Lett.* **86**, 3209 (2001); A. W. Sandvik, *Phys. Rev. B* **66**, 024418 (2002).
- ¹⁷ R. Yu, T. Roscilde, and S. Haas, *Phys. Rev. Lett.* **94**, 197204 (2005).
- ¹⁸ N. Willenbacher and H. Spiering, *J. Phys. C* **21**, 1423 (1988); *J. Phys.: Condens. Matter* **1**, 10089 (1989).
- ¹⁹ O. Waldmann, J. Hassmann, P. Müller, G. S. Hanan, D. Volkmer, U. S. Schubert, and J.-M. Lehn, *Phys. Rev. Lett.* **78**, 3390 (1997).
- ²⁰ C. Boskovic, A. Sieber, G. Chaboussant, H. U. Güdel, J. Ensling, W. Wernsdorfer, A. Neels, G. Labat, H. Stoeckli-Evans, and S. Janssen, *Inorg. Chem.* **43**, 5053 (2004).
- ²¹ T. Lancaster, S. J. Blundell, F. L. Pratt, M. L. Brooks, J. L. Manson, E. K. Brechin, C. Cadiou, D. Low, E. J. L. McInnes, and R. E. P. Winpenny, *J. Phys.: Condens. Matter* **16**, S4563 (2004).
- ²² S. Ferlay, T. Mallah, R. Ouahès, P. Veillet, and M. Verdaguer, *Nature* **378**, 701 (1995).
- ²³ M. Nishino, K. Yamaguchi, and S. Miyashita, *Phys. Rev. B* **58**, 9303 (1998).
- ²⁴ M. Nishino and S. Miyashita, *Phys. Rev. B* **63**, 174404 (2001).
- ²⁵ M. Nishino, K. Boukhechdaden, S. Miyashita, and F. Varret, *cond-mat/0505702* (2005).
- ²⁶ K. Boukhechdaden, M. Nishino, S. Miyashita, and F. Varret, *cond-mat/0505701* (2005).
- ²⁷ C. Timm and U. Schollwöck, *Phys. Rev. B* **71**, 224414 (2005).
- ²⁸ U. Schollwöck, *Rev. Mod. Phys.* **77**, 259 (2005).
- ²⁹ Y. Garcia, O. Kahn, J.-P. Ader, A. Buzdin, Y. Meurdesoif, and M. Guillot, *Phys. Lett. A* **271**, 145 (2000).
- ³⁰ J. Wajnflasz, *J. Phys. Status Solidi* **40**, 537 (1970); J. Wajnflasz and R. Pick, *J. Phys. (Paris), Colloq.* **32**, C1-91 (1971).
- ³¹ S. Doniach, *J. Chem. Phys.* **68**, 4912 (1978).
- ³² P. Fulde and I. Peschel, *Adv. Phys.* **21**, 1 (1972).
- ³³ Mapping onto and solving an Ising-type model is superior to the mean-field approximation, which neglects all fluctuations of σ_i and the spins \mathbf{S}_i . In the Ising approximation we treat fluctuations of σ_i and *longitudinal* fluctuations of \mathbf{S}_i exactly and neglect only *transverse* fluctuations of \mathbf{S}_i .
- ³⁴ F. D. M. Haldane, *Phys. Lett.* **A93**, 464 (1983).